Dynamic Graph Neural Networks for Joint Terahertz based Sensing and Communication Optimization in Vehicular Networks

*Xuefei Li, †Mingzhe Chen, ‡Ye Hu, *Zhilong Zhang, *Danpu Liu, and §Shiwen Mao
*Beijing Laboratory of Advanced Information Network, Beijing University of Posts and Telecommunications,
Beijing, 100876, China, Emails: 2013213202@bupt.edu.cn, zhilong.zhang@outlook.com, dpliu@bupt.edu.cn.
†Department of Electrical and Computer Engineering and Institute for Data Science and Computing, University of Miami,
Coral Gables, FL, 33146, USA, Email: mingzhe.chen@miami.edu.
‡Department of Industrial and System Engineering, University of Miami, Coral Gables, FL, 33146, USA, Email: yehu@miami.edu.
§Department of Electrical and Computer Engineering, Auburn University, Auburn, AL 36849 USA, Email: smao@ieee.org.

2024 IEEE Wireless Communications and Networking Conference (WCNC) | 979-8-3503-0358-2/24/$31.00 ©2024 IEEE | DOI: 10.1109/WCNC57260.2024.10570754

***Abstract*—In this paper, the problem of vehicle service mode selection (sensing, communication, or both) and vehicle connections within terahertz (THz) enabled joint sensing and communications over vehicular networks is studied. The considered network consists of several service provider vehicles (SPVs) that can provide: 1) only sensing service, 2) only communication service, and 3) both services, sensing service request vehicles, and communication service request vehicles. Based on the vehicle network topology and their service accessibility, SPVs strategically select service request vehicles to provide sensing, communication, or both services. This problem is formulated as an optimization problem, aiming to maximize the number of successfully served vehicles by jointly determining the service mode of each SPV and its associated vehicles. To solve this problem, we propose a dynamic graph neural network (GNN) model that selects appropriate graph information aggregation functions according to the vehicle network topology, thus extracting more vehicle network information compared to traditional static GNNs that use fixed aggregation functions for different vehicle network topologies. Using the extracted vehicle network information, the service mode of each SPV and its served service request vehicles will be determined. Simulation results show that the proposed dynamic GNN based scheme can improve the number of successfully served vehicles by up to 17% compared to a GNN based algorithm with a fixed neural network model.**

I. Introduction

Since the joint design of wireless sensing and communications on a single hardware platform can improve spectral efficiency and reduce hardware complexity, it is considered as a promising technology to support various vehicular applications (e.g., autonomous driving and vehicle platooning) [1]. The shortage of wireless spectrum in sub-6 GHz band can substantially constraint the performance of the joint sensing and communication services [2], especially for the vehicular applications where the densely deployed moving vehicles request frequent joint sensing and communication services. This leads us to the usage of high frequency band spectrum, especially to the usage of wider, extra high data rate terahertz (THz) band. However, the sensing and communication signals transmitted in THz bands experiences much higher path loss and are highly vulnerable to blockages [3]. Therefore, deploying THz-enabled vehicular networks to offer high-reliability sensing and communication services faces many challenges such as compensation for severe path loss, reduction of link blockages, and adaptation to dynamic vehicle network topology.

Recently, several works, such as [4]–[6], have studied the problems related to the use of radio frequency for both communications and sensing over vehicular networks. In [4], the authors optimized time slot allocations for sensing and communication services. The work in [5] designed a radar-assisted beamforming scheme while considering the mobility of vehicles. In [6], the authors achieved high-efficient communication and obstacle detection for urban autonomous vehicles by considering the channel sparsity characteristics of the joint communication and sensing systems. However, the methods in [4]–[6] may not be able to capture the dynamics of vehicle network topologies caused by vehicle movements and dynamic wireless channels. In fact, vehicle network topology information can improve both sensing and communication services since it includes the connectivity information of all vehicles, which is crucial for managing the interference between sensing and communication links. To address this challenge, the works in [7]–[10] used graph neural networks (GNNs) to extract topological and geographical location information of dynamic vehicle networks. However, most of these works [7]–[10] used a single predefined GNN model for vehicle information extraction. Hence they did not consider whether the defined GNN model can process various vehicle network topologies thus reducing the information extracted by GNNs.

The main contribution of this work is a novel framework that enables service provider vehicles (SPVs) to efficiently provide sensing and communication services to service request vehicles using THz bands. The considered model consists of several SPVs, communication service request vehicles, and sensing service request vehicles. SPVs provide sensing, communication, or both services to service request vehicles. Therefore, the problem is to determine the service mode (i.e., provide sensing, communication, or both services) of each SPV and its served service request vehicles. This problem is formulated as an optimization problem whose goal is to maximize the total number of successfully served vehicles. To solve this problem, we propose a dynamic GNN that selects appropriate graph information aggregation functions according to the vehicle network topology, thus extracting more vehicle network information compared to traditional static GNNs that use fixed aggregation functions for different vehicle network topology. Using the extracted vehicle network information, the service mode of each SPV and its served service request vehicles will be determined. Simulation results show that the dynamic GNN scheme can improve the number of successfully served vehicles by up to 17% compared to a GNN method with a fixed model.

II. System Model and Problem Formulation

We consider a vehicular network that consists of a set $\mathcal{M}$ of M communication service request vehicles, a set $\mathcal{N}$ of N

This work is supported in part by the National Natural Science Foundation of China under Grant 62271065 and U22B2001, and the Project of China Railway Corporation under Grant N2022G048.

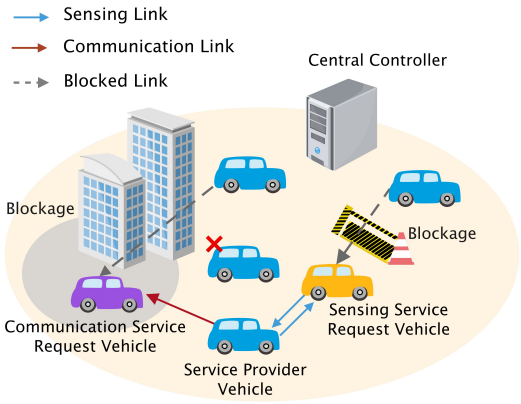

Fig. 1. Illustration of the considered vehicular network model.

sensing service request vehicles, and a set $\mathcal{U}$ of U SPVs. In this network, each SPV uses the same range of THz bands to provide: 1) sensing services, 2) communication services, or 3) both sensing and communication services. As shown in Fig. 1, the wireless links connecting the moving vehicles can be blocked by buildings, which changes the accessibility of each SPV at different service request vehicles. Next, to model the accessibility of the SPVs, we introduce the vehicle blockage model, communication model, and sensing model.

A. Vehicle Blockage Model

The projection of a building on the ground is modeled as a quadrilateral. For a given SPV u, the transmission link between SPV u and communication service request vehicle m will be blocked when the line segment between SPV u and communication service request vehicle m intersects with one of diagonals of the quadrilateral. To have an intersection of the diagonal and the line segment between SPV u and communication service request vehicle m, it needs to satisfy i) SPV u and communication service request vehicle m are on the different sides of the diagonal, ii) the vertices of the diagonal are on the different sides of the straight line passing through SPV u and communication service request vehicle m. Then, we use a binary variable ρ^{C}_{um} to indicate whether a blockage exists between SPV u and communication service request vehicle m: $\rho^{\mathrm{C}}_{um} = 1$ means that the communication link between SPV u and communication service request vehicle m is LoS; otherwise, we have $\rho^{\mathrm{C}}_{um} = 0$. Similarly, a binary variable ρ^{S}_{un} is used to indicate whether a blockage exists between SPV u and sensing service request vehicle n: $\rho^{\mathrm{S}}_{un} = 1$ means that the sensing link between SPV u and sensing service request vehicle n is LoS; otherwise, we have $\rho^{\mathrm{S}}_{un} = 0$.

B. Communication Model

We consider a practical vehicle network where each SPV may not always provide sensing/communication service, such that each vehicle has two states: i) active state in which the SPV can provide services and ii) deactivate state in which the SPV cannot provide any service. Let ω_u be the state of an SPV, where $\omega_u = 1$ indicates that vehicle u can provide sensing, communication, or both services; otherwise, we have $\omega_u = 0$. The probability of an SPV in the active state is p.

The power transmitted by SPV u and received by communication service request vehicle m is $S_{um} = \frac{\omega_u \rho^{\mathrm{C}}_{um} P_u A^{\mathrm{T}}_{um} A^{\mathrm{R}}_{mu}}{H^{\mathrm{F}}_{um} H^{\mathrm{B}}_{um}}$, where P_u is the transmit power of SPV u, H^{F}_{um} is the free space path gain, $H^{\mathrm{B}}_{um} = \frac{1}{r(d_{um})}$ is the molecular absorption path gain with $r(d_{um}) \approx e^{-\tau(f) d_{um}}$ being the transmittance of the medium, $\tau(f)$ is the overall absorption coefficient of the medium, f is the operating frequency, and d_{um} is the distance between SPV u and communication service request vehicle m. Since the molecular absorption H^{B}_{um} and free space path loss H^{F}_{um} lead to the severe attenuation, higher antenna gains are required in the THz bands so as to compensate the severe path loss. The effective THz antenna gain can be represented as a function of the horizontal and vertical beamwidths. Let A^{T}_{um} represent the effective antenna gain of SPV u transmitting data to communication service request vehicle m, which can be denoted by $A^{\mathrm{T}}_{um} = \frac{4\pi}{(\iota+1)\Gamma_{\varrho_u,\varsigma_u}}$ for the main lobe and $A^{\mathrm{T}}_{um} = \frac{4\pi\iota}{(\iota+1)(4\pi-\Gamma_{\varrho_u,\varsigma_u})}$ for the side lobes. Similarly, A^{R}_{mu} represents the effective antenna gain of communication service request vehicle m served by SPV u, which can be denoted by $A^{\mathrm{R}}_{mu} = \frac{4\pi}{(\iota+1)\Gamma_{\varrho_m,\varsigma_m}}$ for the main lobe and $A^{\mathrm{R}}_{mu} = \frac{4\pi\iota}{(\iota+1)(4\pi-\Gamma_{\varrho_m,\varsigma_m})}$ for the side lobes. Here, $\Gamma_{\varrho_u,\varsigma_u} = 4\arcsin\left(\tan\left(\frac{\varrho_u}{2}\right)\tan\left(\frac{\varsigma_u}{2}\right)\right)$, within which ϱ_u and ς_u represent, respectively, the horizontal and vertical beamwidths of the antenna of SPV u. ι captures the side lobe power to main lobe power ration.

The interference of communication service request vehicle m served by SPV u is

$$
\begin{aligned}
Z^{\mathrm{C}}_{um}(\boldsymbol{\alpha},\boldsymbol{\beta}) = &\sum_{i\in\mathcal{U}\setminus\{u\}}\sum_{m'\in\mathcal{M}} \frac{\omega_i \rho^{\mathrm{C}}_{im'} \rho^{\mathrm{C}}_{im} \alpha_{im'} P_i A^{\mathrm{T}}_{im} A^{\mathrm{R}}_{mi}}{H^{\mathrm{B}}_{im} H^{\mathrm{F}}_{im}} \\
&+ \sum_{i\in\mathcal{U}\setminus\{u\}}\sum_{n'\in\mathcal{N}} \frac{\omega_i \rho^{\mathrm{S}}_{in'} \rho^{\mathrm{C}}_{im} \beta_{in'} P_i A^{\mathrm{T}}_{im} A^{\mathrm{R}}_{mi}}{H^{\mathrm{B}}_{im} H^{\mathrm{F}}_{im}} \\
&+ \sum_{n'\in\mathcal{N}} \frac{\omega_u \rho^{\mathrm{S}}_{un'} \rho^{\mathrm{C}}_{um} \beta_{un'} P_u A^{\mathrm{T}}_{um} A^{\mathrm{R}}_{mu}}{H^{\mathrm{B}}_{um} H^{\mathrm{F}}_{um}},
\end{aligned} \tag{1}
$$

where $\boldsymbol{\alpha} = [\boldsymbol{\alpha}_1, \cdots, \boldsymbol{\alpha}_M]$ is communication service vehicle connection indicator matrix with $\boldsymbol{\alpha}_m = [\alpha_{1m}, \cdots, \alpha_{Um}]$, and $\boldsymbol{\beta} = [\boldsymbol{\beta}_1, \cdots, \boldsymbol{\beta}_N]$ is sensing service vehicle connection indicator matrix with $\boldsymbol{\beta}_n = [\beta_{1n}, \cdots, \beta_{Un}]$. $\alpha_{im} = 1$ represents that SPV i is selected to serve communication service request vehicle m in the communication mode; otherwise, $\alpha_{im} = 0$. Similarly, $\beta_{in} = 1$ represents that SPV i is selected to detect sensing service request vehicle n in the sensing mode; otherwise, $\beta_{in} = 0$. Notice that the first two terms of (1) capture, respectively, the interference caused by other communication services, and the interference caused by other sensing services. The third term is the interference caused by the current SPV when it simultaneously provides sensing services. Here, we assume that the transmitter and receiver antenna arrays of an SPV are appropriately designed and achieve isolation as low as -70 dB, hence, the interference caused by communication transmitting antenna to sensing receiving antenna of the same SPV can be ignored [11].

The signal-to-interference-plus-noise ratio (SINR) of communication service request vehicle m served by SPV u

is $\lambda_{um}^{\mathrm{C}}(\boldsymbol{\alpha},\boldsymbol{\beta}) = \frac{S_{um}}{Z_{um}^{\mathrm{C}}(\boldsymbol{\alpha},\boldsymbol{\beta})+\varepsilon_{um}}$, where $\varepsilon_{um} = \varepsilon_0 + \sum_{i\in\mathcal{U}\setminus\{u\}} \omega_i \rho_{im}^{\mathrm{C}} P_i A_{im}^{\mathrm{T}} A_{mi}^{\mathrm{R}} \left(1 - r\left(d_{im}\right)\right) / H_{im}^{\mathrm{F}}$ with ε_0 being the Johnson-Nyquist noise power. ε_{um} is caused by thermal agitation of electrons and molecular absorption. Therefore, the data rate of the link between SPV u and the communication service request vehicle m is $E_{um}^{\mathrm{C}}(\boldsymbol{\alpha},\boldsymbol{\beta}) = B\log_2\left(1+\lambda_{um}^{\mathrm{C}}(\boldsymbol{\alpha},\boldsymbol{\beta})\right)$ with B being the bandwidth.

C. Sensing Model

The interference of sensing service request vehicle n served by SPV u is

$$\begin{aligned} Z_{un}^{\mathrm{S}}(\boldsymbol{\alpha},\boldsymbol{\beta}) = &\sum_{i\in\mathcal{U}\setminus\{u\}}\sum_{m'\in\mathcal{M}} \frac{\omega_i \rho_{im'}^{\mathrm{C}} \rho_{iu}^{\mathrm{S}} \alpha_{im'} P_i A_{iu}^{\mathrm{T}} A_{ui}^{\mathrm{R}}}{H_{iu}^{\mathrm{B}} H_{iu}^{\mathrm{F}}} \\ &+ \sum_{i\in\mathcal{U}\setminus\{u\}}\sum_{n'\in\mathcal{N}} \frac{\omega_i \rho_{in'}^{\mathrm{S}} \rho_{iu}^{\mathrm{S}} \beta_{in'} P_i A_{iu}^{\mathrm{T}} A_{ui}^{\mathrm{R}}}{H_{iu}^{\mathrm{B}} H_{iu}^{\mathrm{F}}} \\ &+ \sum_{i\in\mathcal{U}\setminus\{u\}}\sum_{m'\in\mathcal{M}} \frac{\omega_i \rho_{im'}^{\mathrm{C}} \rho_{in}^{\mathrm{S}} \alpha_{im'} P_i A_{in}^{\mathrm{T}} A_{nu}^{\mathrm{R}} \kappa_{in} c^2}{(4\pi)^3 f^2 d_{in}^2 d_{un}^2 H_{in}^{\mathrm{B}} H_{un}^{\mathrm{B}}} \\ &+ \sum_{i\in\mathcal{U}\setminus\{u\}}\sum_{n'\in\mathcal{N}} \frac{\omega_i \rho_{in'}^{\mathrm{S}} \rho_{in}^{\mathrm{S}} \beta_{in'} P_i A_{in}^{\mathrm{T}} A_{nu}^{\mathrm{R}} \kappa_{in} c^2}{(4\pi)^3 f^2 d_{in}^2 d_{un}^2 H_{in}^{\mathrm{B}} H_{un}^{\mathrm{B}}}, \end{aligned} \tag{2}$$

where κ_{in} is the radar cross section when SPV i provides sensing service for vehicle n. In (2), the first term indicates the interference caused by other SPVs providing communication services with line-of-sight transmission links. The second term indicates the interference caused by other SPVs providing sensing services with line-of-sight transmission links. The third term indicates the interference caused by other SPVs providing communication services via scattering paths. The last term indicates the interference caused by other SPVs providing sensing services via scattering paths. From (1) and (2), we see that a sensing service request vehicle is interfered by the scattering path interference caused by other service request vehicles. However, the scattering path interference will not interfere communication service request vehicles since sensing services are more sensitive to scattered sensing signals [4]. Given (2), the SINR of sensing service request vehicle n served by SPV u is $\lambda_{un}^{\mathrm{S}}(\boldsymbol{\alpha},\boldsymbol{\beta}) = \frac{P_u A_{un}^{\mathrm{T}} A_{nu}^{\mathrm{R}} (H_{un}^{\mathrm{S}})^{-1} (H_{un}^{\mathrm{B}})^{-1}}{Z_{un}^{\mathrm{S}}(\boldsymbol{\alpha},\boldsymbol{\beta})+\varepsilon_{un}}$ with $H_{un}^{\mathrm{S}} = \frac{(4\pi)^3 f^2 d_{un}^4}{\kappa_{un} c^2}$ being the spreading loss.

D. Successfully Served Vehicles

A successfully served vehicle must have its communication or sensing service requirement satisfied. Let Q_m be the size of the information requested by communication service request vehicle m, the transmission delay between communication service request vehicle m and its associated SPV is $\frac{Q_m}{\sum_{u\in\mathcal{U}} \alpha_{um} E_{um}^{\mathrm{C}}(\boldsymbol{\alpha},\boldsymbol{\beta})}$. Then, the set of successfully served communication service request vehicles is given by

$$\mathcal{B} = \{m | \frac{Q_m}{\sum_{u\in\mathcal{U}} \alpha_{um} E_{um}^{\mathrm{C}}(\boldsymbol{\alpha},\boldsymbol{\beta})} \le D_{max}, \forall m \in \mathcal{M}\}, \tag{3}$$

where $D_{\max}$ is the maximum tolerable delay of the communication service. The set of successfully served sensing service request vehicles is

$$\mathcal{O} = \{n | \sum_{u\in\mathcal{U}} \beta_{un} \lambda_{un}^{\mathrm{S}}(\boldsymbol{\alpha},\boldsymbol{\beta}) \ge \lambda_{min}, \forall n \in \mathcal{N}\}, \tag{4}$$

where λ_{min} is the minimum SINR threshold required by the sensing service.

E. Problem Formulation

The goal is to optimize the service mode (i.e., providing sensing, communication, or both services) of each SPV and its associated vehicles to maximize the number of successfully served vehicles. This optimization problem is formulated as

$$\max_{\boldsymbol{\alpha},\boldsymbol{\beta}} \quad |\mathcal{B}| + |\mathcal{O}| \tag{5}$$

$$\text{s.t.} \quad (3) - (4), \tag{5a}$$

$$\sum_{u\in\mathcal{U}} \alpha_{um} = 1, \alpha_{um} \in \{0,1\}, \forall m \in \mathcal{M}, \tag{5b}$$

$$\sum_{u\in\mathcal{U}} \beta_{un} = 1, \beta_{un} \in \{0,1\}, \forall n \in \mathcal{N}, \tag{5c}$$

where $|\mathcal{B}|$ is the number of successfully served communication service request vehicles, and $|\mathcal{O}|$ is the number of successfully served sensing service request vehicles. In (5), constraint (5b) requires a communication service request vehicle to be served by only one SPV. Constraint (5c) requires a sensing service request vehicle to be served by only one SPV.

Problem (5) is hard to solve due to the following reasons. Traditional optimization methods require accurate channel information to obtain the free space path gain H_{um}^{F} and molecular absorption path gain H_{um}^{B} to solve problem (5). However, only periodically reported channel information can be obtained in highly dynamic THz-enabled vehicular networks, which leads to low efficiency in service mode selection and service vehicle connection. To solve this problem, we use a dynamic GNN model [12] to extract each vehicle's graph information related to its location, connection, and interference, rather than simply using the inaccurate channel information.

III. Dynamic GNN based Solution

In this section, a dynamic GNN based algorithm is introduced to solve problem (5). We first introduce graph representation of the considered vehicular networks. Then, we present the components of the GNN based algorithm and the training process. Finally, we provide the entire procedure of using the proposed algorithm to select vehicle service mode and determine the service request vehicle connection.

A. Graph Representation for Vehicular Networks

We first introduce the representation of the considered vehicular network using a graph. Each vehicle is modeled as a node while each connected link (e.g., sensing link, communication link, and interference link) between two vehicles is modeled as an edge. Let $\mathcal{G} = (\mathcal{V}, \mathcal{E})$ represent a graph with node features $\boldsymbol{f} \in \mathbb{R}^{P\times|\mathcal{V}|}$, where $\mathcal{V}$ and $\mathcal{E}$ represent the node and edge sets, respectively. The node set $\mathcal{V} = \mathcal{U} \cup \mathcal{M} \cup \mathcal{N}$ contains three types of vehicles, $|\mathcal{V}| = U + M + N$ is the number of vehicles, and $P = U + 2(M + N)$ is the dimension of node features. Specifically, the node features can be defined by $\boldsymbol{f} = [\boldsymbol{f}_1, \cdots, \boldsymbol{f}_V]$ with $\boldsymbol{f}_v = [e_{v1}, \ldots, e_{vM'}, g_{v1}, \ldots, g_{vV}]^{\top}$ being the node feature for vehicle $v \in \mathcal{V}$, where $e_{vm'}$ is the number of SPVs within the LoS link between vehicle v and vehicle m', $g_{vv'} = \left(H_{vv'}^{\mathrm{B}} H_{vv'}^{\mathrm{F}}\right)^{-1}$ is the free space and

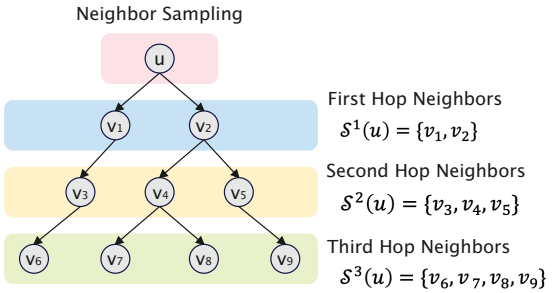

Fig. 2. Neighbor sampling process of vehicle u.

molecular absorption path gain between vehicle v and v', and $\mathcal{M}' = \mathcal{M} \cup \mathcal{N}$ is the set of service request vehicles. Moreover, we assume that there is an edge between SPV u and service request vehicle m' when $\omega_u \rho_{um'} = 1$, which guarantees that the SPV u is working in an active state and the connected link between SPV u and service request vehicle m' is not blocked. Since the locations and working state of vehicles vary over time, the edge set $\mathcal{E}$ will change dynamically in different vehicle topologies.

For each vehicle u, we define three types of vehicles as follows: 1) the first hop vehicles which can directly connect to vehicle u are represetned by $\mathcal{S}^1(u) = \{v \in \mathcal{V} | (u, v) \in \mathcal{E}\}$ with $|\mathcal{S}^1(u)|$ being the number of vehicles in set $\mathcal{S}^1(u)$, 2) the second hop vehicles which can connect to vehicle u via the first hop vehicles are represented by $\mathcal{S}^2(u) = \{\mathcal{S}^1(v) | v \in \mathcal{S}^1(u)\}$ with $|\mathcal{S}^2(u)|$ being the number of vehicles in $\mathcal{S}^2(u)$, and 3) the third hop vehicles which can connect to vehicle u via the second hop vehicles are represented by $\mathcal{S}^3(u) = \{\mathcal{S}^1(v) | v \in \mathcal{S}^2(u)\}$ with $|\mathcal{S}^3(u)|$ being the number of vehicles in $\mathcal{S}^3(u)$. For the example shown in Fig. 2, we have $\mathcal{S}^1(u) = \{v_1, v_2\}$, $\mathcal{S}^2(u) = \{v_3, v_4, v_5\}$, and $\mathcal{S}^3(u) = \{v_6, v_7, v_8, v_9\}$.

B. Components of the GNN based Algorithm

As shown in Fig. 3, the components of the proposed GNN based algorithm are [12]: 1) input layer, 2) hidden layer hidden layer I, 3) hidden layer II, 4) hidden layer III, 5) hidden layer IV, 6) hidden layer V-VII, and 7) output layer. These components are specified as follows:

- *Input*: The input of the proposed GNN model is connected to two paralleled fully connected layers (FCLs). The input of the first fully connected layer is $\boldsymbol{h}_u^0 = \boldsymbol{f}_u \in \mathbb{R}^{P \times 1}$ and the input of the second fully connected layer is $\boldsymbol{h}_{\mathrm{L}}^1 \in \mathbb{R}^{P \times 1}$, where

$$\boldsymbol{h}_{\mathrm{L}}^1 = \frac{1}{|\mathcal{S}^1(u)|} \sum_{v' \in \mathcal{S}^1(u)} \boldsymbol{h}_{v'}^0, \tag{6}$$

  with $\boldsymbol{h}_{v'}^0 = \boldsymbol{f}_{v'} \in \mathbb{R}^{P \times 1}$.
- *Hidden Layer I*: This layer consists of two paralleled FCLs and it is used to extract the graph information of first hop vehicles of each vehicle u. The output of this layer is

$$\boldsymbol{h}_u^1 = \sigma\left(\left[\boldsymbol{w}_1 \boldsymbol{h}_u^0 \| \boldsymbol{w}_2 \boldsymbol{h}_{\mathrm{L}}^1\right]\right), \tag{7}$$

  where $\sigma(\cdot)$ is the rectified linear unit function, $\cdot\|\cdot$ being the vector concatenation, $\boldsymbol{w}_1 \in \mathbb{R}^{(\Omega_0/2) \times P}$ and $\boldsymbol{w}_2 \in \mathbb{R}^{(\Omega_0/2) \times P}$ are the weight parameters of the two FCLs, and Ω_0 is the dimension of graph information vector. We define (6) and (7) as a node aggregation function that is used to extract the graph information of vehicle u. We can also consider other types of node aggregation functions as shown in Table XI of [12]. Since (6) and (7) extract the graph information of only vehicle u and we need the graph information $\boldsymbol{h}_{v'}^1$ of all sampled first hop vehicles to optimize mode selection and vehicle connection, we need to implement (6) and (7) for $|\mathcal{S}^1(u)|$ times.
- *Hidden Layer II*: This layer consists of two paralleled FCLs and it is used to extract the graph information of second hop vehicles of each vehicle u. The input of the first fully connected layer is $\boldsymbol{h}_u^1 \in \mathbb{R}^{\Omega_0 \times 1}$ and the input of the second fully connected layer is $\boldsymbol{h}_{\mathrm{L}}^2 \in \mathbb{R}^{\Omega_0 \times 1}$, where

$$\boldsymbol{h}_{\mathrm{L}}^2 = \frac{1}{|\mathcal{S}^1(u)|} \sum_{v' \in \mathcal{S}^1(u)} \boldsymbol{h}_{v'}^1. \tag{8}$$

  Then, the output of this layer is

$$\boldsymbol{h}_u^2 = \sigma\left(\left[\boldsymbol{w}_3 \boldsymbol{h}_u^1 \| \boldsymbol{w}_4 \boldsymbol{h}_{\mathrm{L}}^2\right]\right), \tag{9}$$

  where $\boldsymbol{h}_u^2 \in \mathbb{R}^{\Omega_0 \times 1}$, $\boldsymbol{w}_3 \in \mathbb{R}^{(\Omega_0/2) \times \Omega_0}$ and $\boldsymbol{w}_4 \in \mathbb{R}^{(\Omega_0/2) \times \Omega_0}$ are the weight parameters of the two FCLs, respectively. Similarly, (8) and (9) are also a node aggregation function that is used to extract the graph information of vehicle u and its second hop neighbors. To obtain the the graph information $\boldsymbol{h}_{v'}^2$ of all sampled vehicles in $\mathcal{S}^1(u)$ to optimize mode selection and vehicle connection, we need to implement (8) and (9) for $|\mathcal{S}^1(u)|$ times.
- *Hidden Layer III*: This layer consists of two paralleled FCLs and it is used to extract the graph information of third hop vehicles of each vehicle u. The input of the first fully connected layer is $\boldsymbol{h}_u^2 \in \mathbb{R}^{\Omega_0 \times 1}$ and the input of the second fully connected layer is $\boldsymbol{h}_{\mathrm{L}}^3 \in \mathbb{R}^{\Omega_0 \times 1}$, where

$$\boldsymbol{h}_{\mathrm{L}}^3 = \frac{1}{|\mathcal{S}^1(u)|} \sum_{v' \in \mathcal{S}^1(u)} \boldsymbol{h}_{v'}^2. \tag{10}$$

  Then, the output of this layer is

$$\boldsymbol{h}_u^3 = \sigma\left(\left[\boldsymbol{w}_5 \boldsymbol{h}_u^2 \| \boldsymbol{w}_6 \boldsymbol{h}_{\mathrm{L}}^3\right]\right), \tag{11}$$

  where $\boldsymbol{h}_u^3 \in \mathbb{R}^{\Omega_0 \times 1}$, $\boldsymbol{w}_5 \in \mathbb{R}^{(\Omega_0/2) \times \Omega_0}$ and $\boldsymbol{w}_6 \in \mathbb{R}^{(\Omega_0/2) \times \Omega_0}$ are the weight parameters of the two FCLs, respectively. Similarly, (10) and (11) are also a node aggregation function that is used to extract the graph information of vehicle u and its third hop neighbors.
- *Hidden Layer IV*: This layer consists of three paralleled FCLs and it is used to combine the output of hidden layers I-III (i.e., $\boldsymbol{h}_u^1$, $\boldsymbol{h}_u^2$, and $\boldsymbol{h}_u^3$). The output of the this layer is the graph information vector $\boldsymbol{h}_u^4 \in \mathbb{R}^{\lambda_0 \times 1}$ of vehicle u, which can be expressed as

$$\boldsymbol{h}_u^4 = \sigma\left(\left[\boldsymbol{w}_7 \boldsymbol{h}_u^1 \| \boldsymbol{w}_8 \boldsymbol{h}_u^2 \| \boldsymbol{w}_9 \boldsymbol{h}_u^3\right]\right), \tag{12}$$

  where $\boldsymbol{w}_7 \in \mathbb{R}^{(\Omega_0/3) \times \Omega_0}$, $\boldsymbol{w}_8 \in \mathbb{R}^{(\Omega_0/3) \times \Omega_0}$, and $\boldsymbol{w}_9 \in \mathbb{R}^{(\Omega_0/3) \times \Omega_0}$ are the weight parameters for the output of hidden layers I-III , respectively. Here, the output $\boldsymbol{h}_u^4$ can

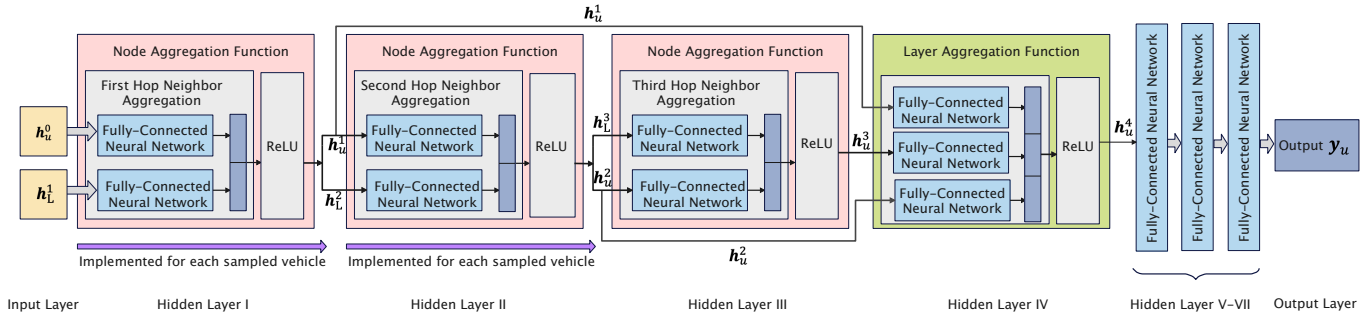

Fig. 3. Structure of the proposed GNN model.

be considered as the final graph information of vehicle u, since it includes the graph information of sampled first hop, second hop, and third hop vehicles. We define (12) as a layer aggregation function that is used to combine the output of the node aggregation functions in (7), (9), and (11) for vehicle u. We can also consider other types of layer aggregation functions as shown in Table I of [12].

- *Hidden Layer V-VII*: This layer consists of three cascaded FCLs. It is used to find the relationship between the graph information vector $\boldsymbol{h}_u^4$ and the probability distribution of vehicle u providing service for each service request vehicle in the corresponding sensing or communication mode.
- *Output*: The output is the probability distribution of vehicle u serving $M+N$ service request vehicles in the corresponding sensing or communication mode and it is represneted by $\boldsymbol{y}_u = \left[y_u^1, \cdots, y_u^{M+N+1}\right]$. It includes the case that SPV u does not serve any service request vehicles, and hence, we have $\boldsymbol{y}_u \in \mathbb{R}^{(M+N+1)\times 1}$. Based on the probability distribution $\boldsymbol{y}_u$ of each vehicle u, the service mode selection and service request vehicle connection of each SPV is determined by selecting the vehicle with the highest probability. Here, the designed GNN model can be applied for a network in which M and N are constant. If M or N in the network changes, we only need to train hidden layers V-VII. This is because hidden layers I-IV are used a fixed number of vehicles to extract the feature of each vehicle.

C. Training the GNN based Algorithm

Next, we first introduce the process of finding appropriate aggregation functions for the proposed GNN based method. Then, we define the loss function and explain the entire training procedure. To find the appropriate node and layer aggregation functions for different vehicle topologies, we define a trainable vector $\boldsymbol{\theta} \in \mathbb{R}^{(KA_1+A_2)\times 1}$, which represents the probabilities of selecting each node aggregation function and layer aggregation function, where A_1 is the number of the node aggregation functions that the GNN can select, A_2 is the number of the layer aggregation functions that the GNN can select, and K is the number of node aggregation functions used in the proposed GNN based method. From the definition of $\boldsymbol{\theta}$, it is actually used to select K node aggregation functions and one layer aggregation function. We then use binary cross entropy (BCE) to capture the difference between the predicted and actual service request vehicle connection results, which is

$$\begin{aligned}\mathcal{J}\left(\boldsymbol{w},\boldsymbol{\theta}\right) = \sum_{i=1}^{M+N+1} & -z_u^i \log \delta\left(y_u^i\left(\boldsymbol{w},\boldsymbol{\theta}\right)\right) \\ & -\left(1-z_u^i\right)\log\left(1-\delta\left(y_u^i\left(\boldsymbol{w},\boldsymbol{\theta}\right)\right)\right),\end{aligned} \tag{13}$$

where $\delta(\cdot)$ is the sigmoid function, z_u^i is the label of vehicle u in class i which indicates that vehicle u is selected to serve service request vehicle i, and $\boldsymbol{w}$ is a vector of all GNN parameters.

Given (13), we then show how to train the proposed GNN model. The proposed GNN method is trained with an iterative method that consists of two steps: 1) Joint optimization of $\boldsymbol{\theta}$ and $\boldsymbol{w}$, and 2) optimization of $\boldsymbol{w}$ given $\boldsymbol{\theta}$. Specifically, the two steps are elaborated as follows:

1) Joint optimization of $\boldsymbol{\theta}$ and $\boldsymbol{w}$: Let $\mathcal{J}_{\text{tra}}\left(\boldsymbol{w},\boldsymbol{\theta}\right)$ and $\mathcal{J}_{\text{val}}\left(\boldsymbol{w},\boldsymbol{\theta}\right)$ denote the training and the validation loss, respectively. Then, the goal of optimizing $\boldsymbol{\theta}$ and $\boldsymbol{w}$ is expressed as

$$\min_{\boldsymbol{\theta}} \quad \mathcal{J}_{\text{val}}\left(\boldsymbol{w}^*(\boldsymbol{\theta}),\boldsymbol{\theta}\right) \tag{14}$$

$$\text{s.t.} \quad \boldsymbol{w}^*(\boldsymbol{\theta}) = \text{argmin}_{\boldsymbol{w}}\, \mathcal{J}_{\text{tra}}(\boldsymbol{w},\boldsymbol{\theta}). \tag{14a}$$

Due to the difficulty in finding a closed-form solution for (14a), we solve (14) and (14a) in an iterative manner. Firstly, we explain the process of optimizing $\boldsymbol{\theta}$ based on validation data. To reduce the computational overhead for obtaining $\nabla_{\boldsymbol{\theta}}\mathcal{J}_{\text{val}}\left(\boldsymbol{w}^*(\boldsymbol{\theta}),\boldsymbol{\theta}\right)$ in (14), we use a gradient based approximation method [12] to approximate $\nabla_{\boldsymbol{\theta}}\mathcal{J}_{\text{val}}\left(\boldsymbol{w}^*(\boldsymbol{\theta}),\boldsymbol{\theta}\right)$ by adapting $\boldsymbol{w}$ using only a single training step, which is

$$\nabla_{\boldsymbol{\theta}}\mathcal{J}_{\text{val}}\left(\boldsymbol{w}^*(\boldsymbol{\theta}),\boldsymbol{\theta}\right) \approx \nabla_{\boldsymbol{\theta}}\mathcal{J}_{\text{val}}\left(\boldsymbol{w}-\xi\nabla_{\boldsymbol{w}}\mathcal{J}_{\text{tra}}(\boldsymbol{w},\boldsymbol{\theta}),\boldsymbol{\theta}\right), \tag{15}$$

where ξ is the learning rate. Then, $\boldsymbol{\theta}$ and GNN parameters $\boldsymbol{w}$ are updated by using a standard gradient descent method

By iteratively updating $\boldsymbol{\theta}$ and $\boldsymbol{w}$ until convergence, problem (14) can be solved and the well-trained $\boldsymbol{\theta}^*$ can be obtained.

2) Optimization of $\boldsymbol{w}$ given $\boldsymbol{\theta}^*$: Based on $\boldsymbol{\theta}^*$, the node aggregation functions and layer aggregation function for the GNN are determined. Then, the GNN parameters $\boldsymbol{w}$ is tuned on the validation data to further improve the performance of the proposed method. The update process of $\boldsymbol{w}$ is [13]

$$\boldsymbol{w} \leftarrow \boldsymbol{w} - \mu\nabla_{\boldsymbol{w}}\mathcal{J}_{\text{val}}(\boldsymbol{w},\boldsymbol{\theta}^*), \tag{16}$$

where μ is the learning rate. By updating (16) until convergence, the well-trained $\boldsymbol{w}^*$ can be obtained. Finally, based on

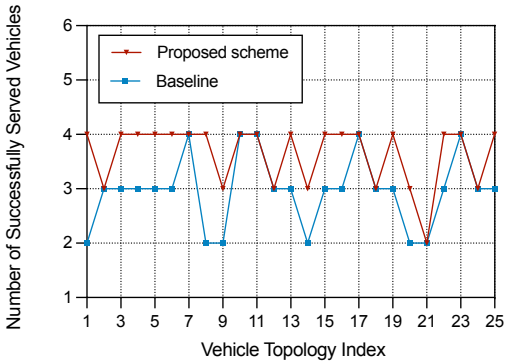

Fig. 4. The number of successfully served vehicles as the vehicle topology varies ($\Omega_0 = 64$, $|\mathcal{S}^1(u)| = |\mathcal{S}^2(u)| = |\mathcal{S}^3(u)| = 10$, $p = 0.9$, $U = 10$, $M = N = 2$, and $Q = 20$MB).

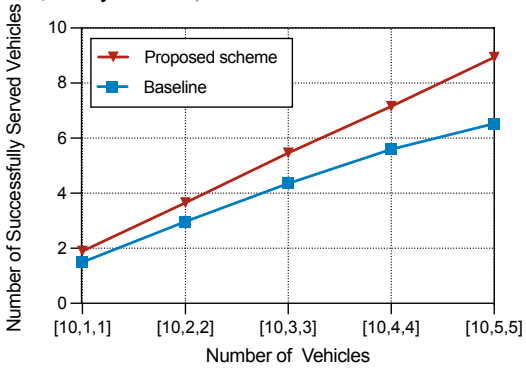

Fig. 5. The number of successfully served vehicles as the number of vehicles varies ($U = 10$, M and N vary from 1 to 5).

the well-trained $\boldsymbol{w}^*$, the optimal probability distribution $\boldsymbol{y}_u$ of determining the service mode selection and service vehicle connection for each SPV can be obtained.

IV. Simulation Results and Analysis

In our simulations, we consider an urban region with the diameter of 100 m. The requirements of sensing and communication services are set as $\lambda_{\min} = 3$dB and $D_{max} = 3$ms, respectively. Other parameters refer to Table II in [3]. The vehicle network topologies are obtained from a Taxi dataset of Shanghai [14]. For comparison, we consider a baseline that uses a standard GNN model with a fixed neural network model.

Fig. 4 shows how the number of successfully served vehicles changes as the vehicle topology varies. From Fig. 4, we see that the proposed scheme improves the number of successfully served vehicles by up to 17% compared to baseline. This is because the proposed scheme selects appropriate aggregation functions for different vehicle network topologies, hence, better graph information vectors can be learned.

Fig. 5 shows how the number of successfully served vehicles changes as the number of vehicles varies. From this figure, we see that, as the number of service request vehicles increases, the number of successfully served vehicles increases since more sensing and communication links are established. Fig. 5 also shows that the proposed scheme can increase the number of successful served vehicles by up to 19.79% compared to baseline. This is because the proposed scheme uses a dynamic GNN model to extract more vehicle network information.

V. Conclusions

In this paper, we have designed a novel framework that uses THz for joint communication and sensing in vehicular networks. Our goal was to maximize the number of successfully served vehicles by jointly determining the service mode of each SPV and the service request vehicles served by each SPV. We formulated an optimization problem that jointly considers service mode, service vehicle connection, THz channel particularities, and dynamic vehicle network topology. To solve this problem, we have designed a novel GNN based method which enables a GNN to select appropriate graph information aggregation functions for different vehicle network topologies thus extracting more vehicle network information and improving the service mode and service request vehicle connection strategy of each SPV. Simulation results verified that the proposed dynamic GNN based method can achieve significant gains compared to the standard GNN based solution.

References

[1] F. Liu, Y. Cui, C. Masouros, J. Xu, T. X. Han, Y. C. Eldar, and S. Buzzi, "Integrated sensing and communications: Toward dual-functional wireless networks for 6G and beyond," *IEEE Journal on Selected Areas in Communications*, vol. 40, no. 6, pp. 1728–1767, June 2022.

[2] W. Saad, M. Bennis, and M. Chen, "A vision of 6G wireless systems: Applications, trends, technologies, and open research problems," *IEEE Network*, vol. 34, no. 3, pp. 134–142, May/June 2020.

[3] A. Shafie, N. Yang, S. Durrani, X. Zhou, C. Han, and M. Juntti, "Coverage analysis for 3D terahertz communication systems," *IEEE Journal on Selected Areas in Communications*, vol. 39, no. 6, pp. 1817–1832, June 2021.

[4] Q. Zhang, H. Sun, X. Gao, X. Wang, and Z. Feng, "Time-division ISAC enabled connected automated vehicles cooperation algorithm design and performance evaluation," *IEEE Journal on Selected Areas in Communications*, vol. 40, no. 7, pp. 2206–2218, July 2022.

[5] D. Cong, S. Guo, S. Dang, and H. Zhang, "Vehicular behavior-aware beamforming design for integrated sensing and communication systems," *IEEE Transactions on Intelligent Transportation Systems*, to appear, 2023, doi:10.1109/TITS.2023.3251303.

[6] H. Ma, Z. Wei, Z. Li, F. Ning, X. Chen, and Z. Feng, "Performance of cooperative detection in joint communication-sensing vehicular network: A data analytic and stochastic geometry approach," *IEEE Transactions on Vehicular Technology*, vol. 72, no. 3, pp. 3848–3863, Mar. 2023.

[7] Z. Wang, Y. Zhou, Y. Zou, Q. An, Y. Shi, and M. Bennis, "A graph neural network learning approach to optimize RIS-assisted federated learning," *IEEE Transactions on Wireless Communications*, to appear, 2023, doi:10.1109/TWC.2023.3239400.

[8] J. Lee, Y. Cheng, D. Niyato, Y. L. Guan, and D. G. González, "Intelligent resource allocation in joint radar-communication with graph neural networks," *IEEE Transactions on Vehicular Technology*, vol. 71, no. 10, pp. 11 120–11 135, Oct. 2022.

[9] L. Zeng, C. Yang, P. Huang, Z. Zhou, S. Yu, and X. Chen, "GNN at the edge: Cost-efficient graph neural network processing over distributed edge servers," *IEEE Journal on Selected Areas in Communications*, vol. 41, no. 3, pp. 720–739, Mar. 2023.

[10] X. Li, M. Chen, Y. Liu, Z. Zhang, D. Liu, and S. Mao, "Graph neural networks for joint communication and sensing optimization in vehicular networks," *IEEE Journal on Selected Areas in Communications*, vol. 41, no. 12, pp. 3893–3907, Dec. 2023.

[11] B. Liu, J. Liu, and N. Kato, "Optimal beamformer design for millimeter wave dual-functional radar-communication based V2X systems," *IEEE Journal on Selected Areas in Communications*, vol. 40, no. 10, pp. 2980–2993, Oct. 2022.

[12] H. Zhao, Q. Yao, and W. Tu, "Search to aggregate neighborhood for graph neural network," in *Proc. IEEE International Conference on Data Engineering (ICDE)*, Chania, Crete, Greece, Apr. 2021, pp. 552–563.

[13] M. Chen, D. Gündüz, K. Huang, W. Saad, M. Bennis, A. V. Feljan, and H. V. Poor, "Distributed learning in wireless networks: Recent progress and future challenges," *IEEE Journal on Selected Areas in Communications*, vol. 39, no. 12, pp. 3579–3605, Dec. 2021.

[14] D. Zhao, Y. Gao, Z. Zhang, Y. Zhang, and T. Luo, "Prediction of vehicle motion based on Markov model," in *Proc. International Conference on Computer Systems, Electronics and Control (ICCSEC)*, Dalian, China, Dec. 2017, pp. 205–209.